Electronic Supplementary Material (ESI) for Inorganic Chemistry Frontiers.


# Supplementary Information

# The Synthesis of Zeolitic Imidazolate Frameworks/Prussian Blue Analogues Heterostructure Composites and Their Application in Supercapacitors

Xinyue Wu,[a] Qingling Jing,[a] Fancheng Sun,[a,b] Huan Pang*[a]

[a.] School of Chemistry and Chemical Engineering, Yangzhou University, Yangzhou, 225009, Jiangsu, P. R. China.

[b.] Interdisciplinary Materials Research Center, Institute for Advanced Study, Chengdu University, Chengdu, 610106, Sichuan, P.R. China.

*Corresponding authors: huanpangchem@hotmail.com; panghuan@yzu.edu.cn

## 1. Experimental section

### 1.1. Synthesis of ZIF-67@PBA nanoparticles

Typically, $Co(NO_3)_2 \cdot 6H_2O$ (0.58 g), and 2-methylimidazole (0.65 g) were dissolved in 20 mL of methanol, respectively. The methanolic solution of $Co(NO_3)_2$ was quickly injected into the solution of 2-methylimidazole at room temperature. After reacting for 20 minutes, the product ZIF-67 was collected by centrifugation and washed by methanol. 20 mg $K_3[Fe(CN)_6]$ and 40 mg ZIF-67 were dispersed into ethanol and water mixed solvent with stirring for 4 h at room temperature. The volume ratio of ethanol and water in the mixed solvent was 9:1, 1:1, 1:2, corresponding to the products ZP1, ZP2, ZP3.

To modulate its microstructure, we calcined ZP composites at different target temperatures (150, 250, 350 $^oC$ under $N_2$ atmosphere for 2 h, obtaining ZP-X (X denoted temperature).

### 1.2 Electrochemical measurements

The electrochemical measurements were carried out with CHI760e working station in 3.0 M KOH solution at room temperature. Galvanostatic charge-discharge (GCD), Cyclic voltammetry (CV) and electrochemical impedance spectroscopy (EIS) were used to evaluate the capacitive properties of the ZIF-67@PBAs. The EIS measurements were conducted in the frequency range of 100 kHz to 0.01 Hz at the open circuit voltage.

For the three-electrode cell, the working electrodes were fabricated by mixing the active materials MOF, acetylene black, and polytetrafluoroethylene in a mass ratio of 80 : 15 : 5. The mixture was ground adequately to form a slurry and coated on nickel foam (≈ 1 $cm^2$ ), then pressed into a thin foil at a pressure of 10 MPa. A platinum electrode and a Hg/HgO electrode were served as the counter and reference electrode, respectively.

For the hybrid supercapacitor cells, the electrochemical measurements were conducted in a two-electrode electrochemical cell with MOF materials as positive electrode and activated carbon (AC) as negative electrode in 3.0 M KOH solution at room temperature. The positive electrode and negative electrode were fabricated by mixing the as-prepared MOF/activated carbon, acetylene black and polytetrauoroethylene at a weight ratio of 80: 15: 5. The mixture was ground

adequately to form a slurry and coated on nickel foam (≈ 1 $cm^2$ ), then pressed into a thin foil at a pressure of 10 MPa.

**1.3 Calculation**

The specific capacitance of the electrode material can be calculated from the charge-discharge curves according to the equation:

$$C=Q / (m \times \Delta V) = \int I\, dt / (m \times \Delta V) = I \times t_{discharge} / (m \times \Delta V)$$

Where C is specific capacitance in F $g^{-1}$ , t $t_{discharge}$ is the discharging time in s, ΔV is the potential window in V.

Table S1 Comparisons of other ZIF-based materials for SCs Sample

| Sample | Electrolyte | Scan rate ($mV\ s^{-1}$) | Current density ($A\ g^{-1}$) | Capacitance ($F\ g^{-1}$) | Ref. |
|---|---|---|---|---|---|
| ZIF-67/PEDOT composite | PVA/1 M $H_2SO_4$ | | 1.0 | 106.8 | [1] |
| ZIF-67/GO-2 composite | 6 M KOH | 0.5 | | 100.4 | [2] |
| P-ZIF-67 | 6 M KOH | | 1.0 | 120.0 | [3] |
| ZIF-67 microflowers | 1 M KOH | | 1.0 | 188.7 | [4] |
| ZP2-250 | 3 M KOH | | 0.5 | 190.7 | This work |

Table S2 The BET properties of the ZP2-X composites

| Sample | $S_{BET}$ [$m^2$ /g] | $V_{micro}$ [$cm^3$/g] |
|---|---|---|
| ZP2 | 511.444 | 0.250 |
| ZP2-150 | 676.417 | 0.313 |
| ZP2-250 | 835.843 | 0.395 |
| ZP2-350 | 627.057 | 0.303 |

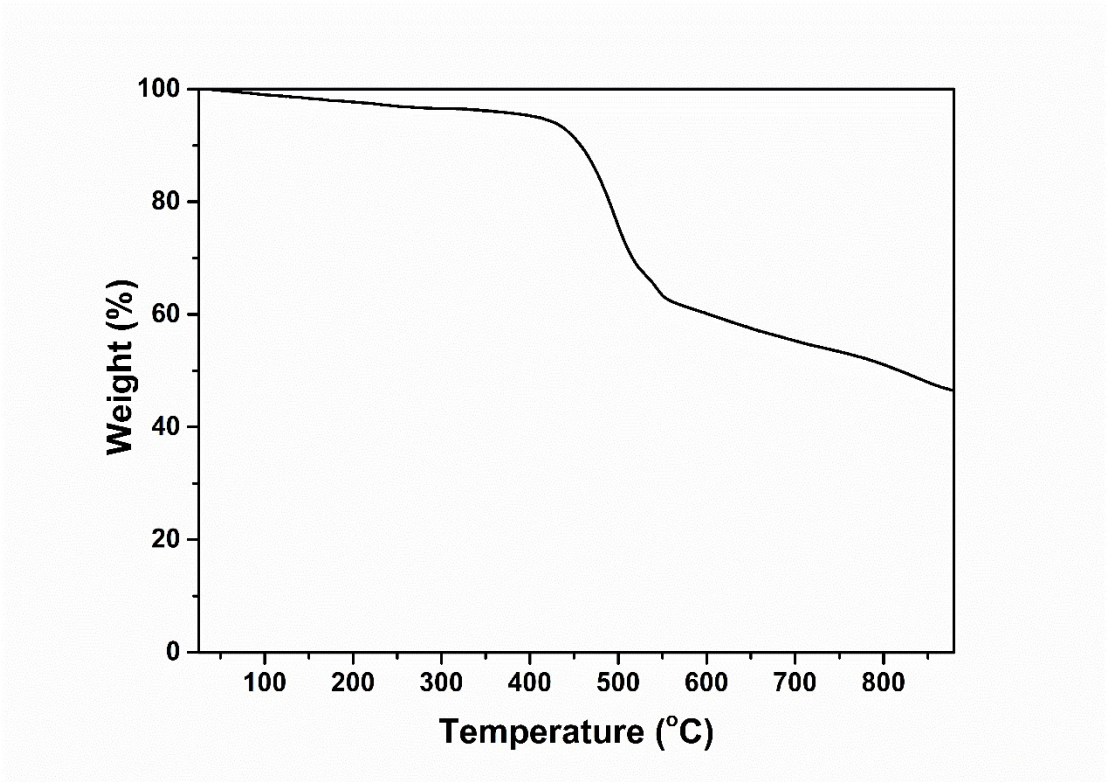


Figure S1 TGA curves of the ZP2 composites under $N_2$ atmosphere.

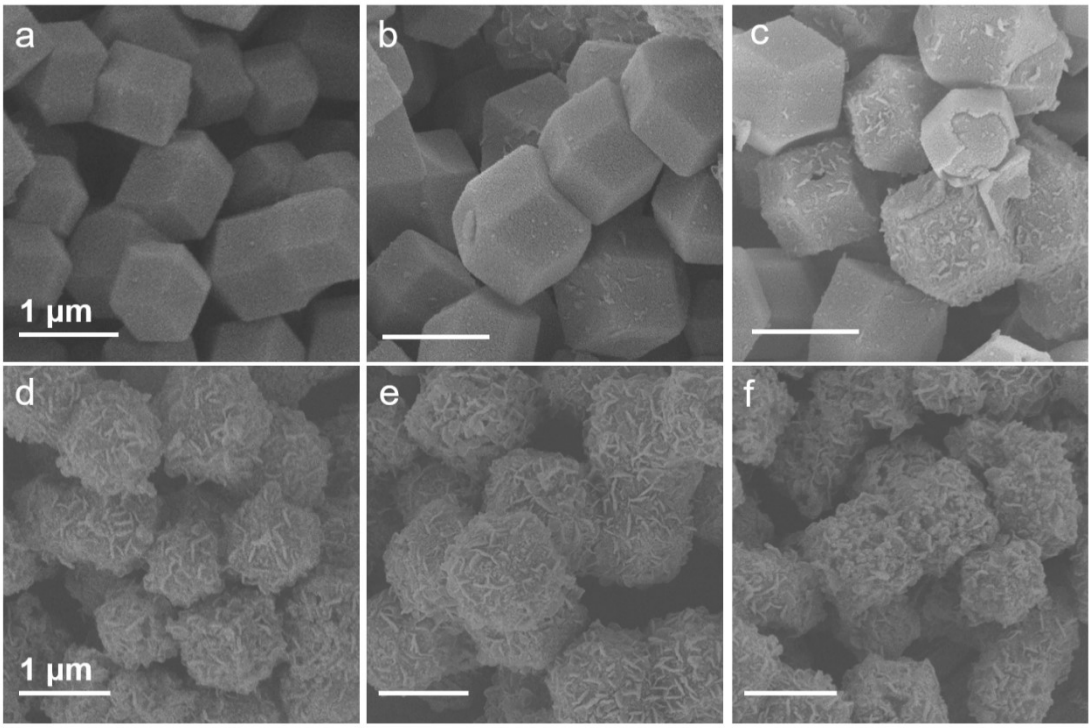


Figure S2 The SEM images of ZP1-150, ZP1-250, ZP1-350, ZP3-150, ZP3-250, ZP3-350 composites.

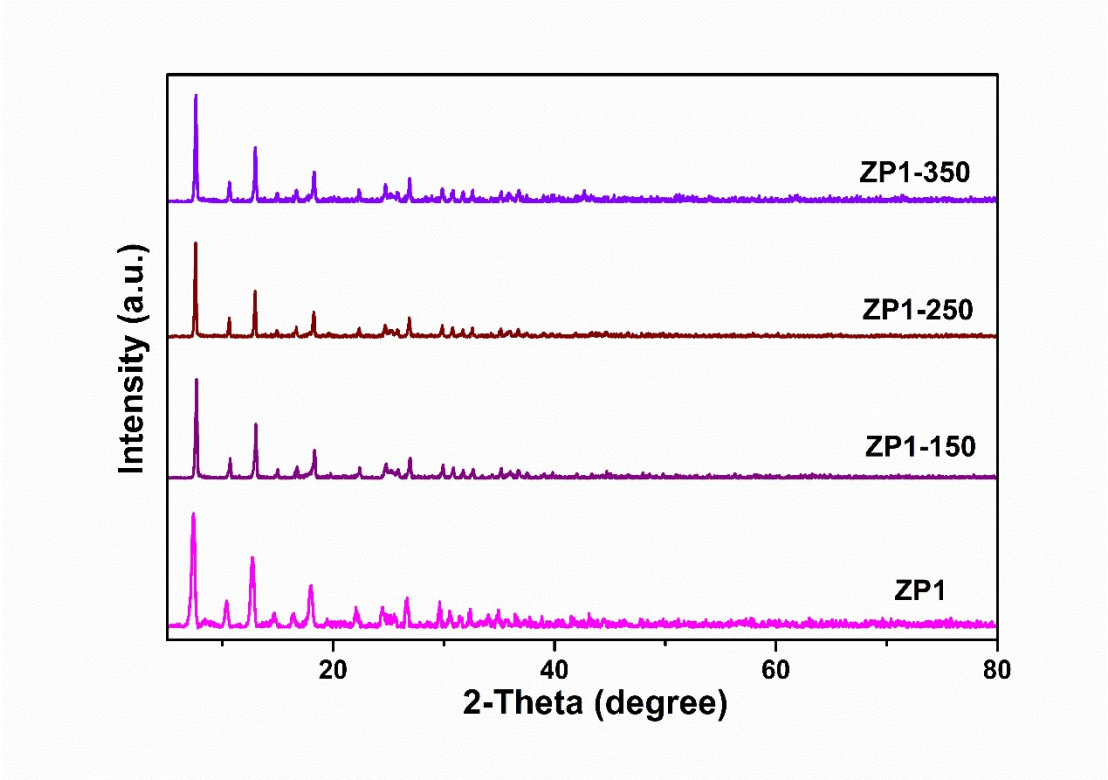


Figure S3 XRD patterns of the ZP1, ZP1-150, ZP1-250, ZP1-350 composites.

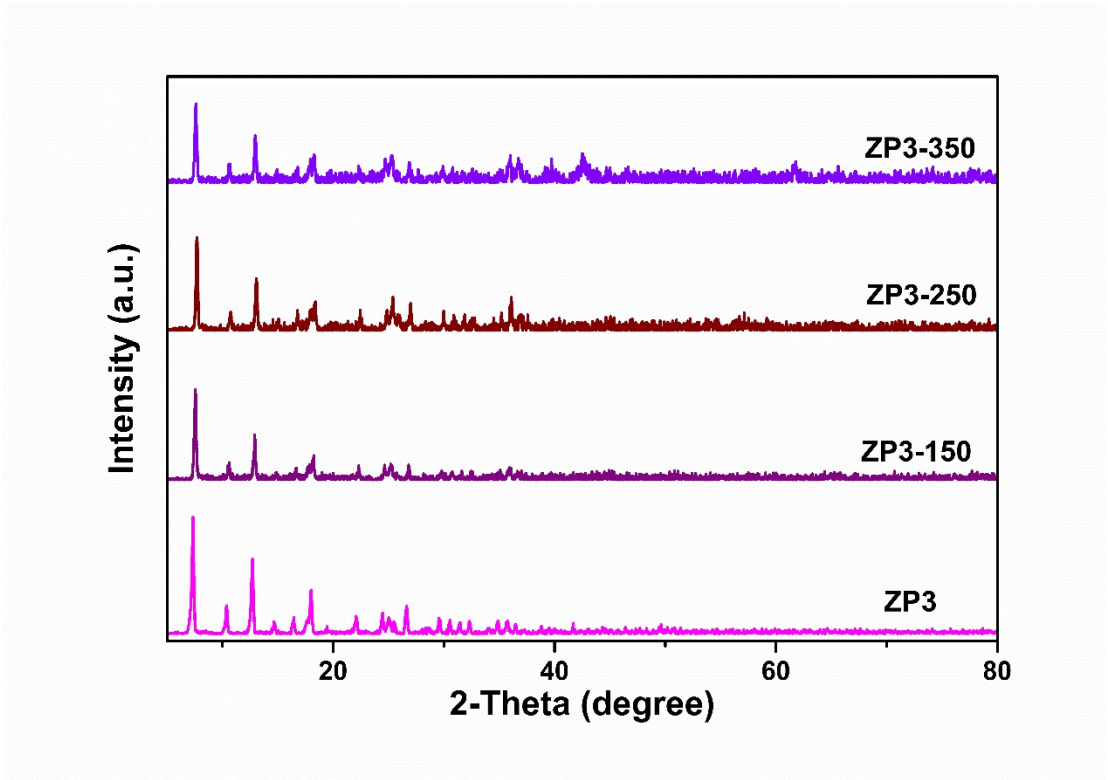


Figure S4 XRD patterns of the ZP3, ZP3-150, ZP3-250, ZP3-350 composites.

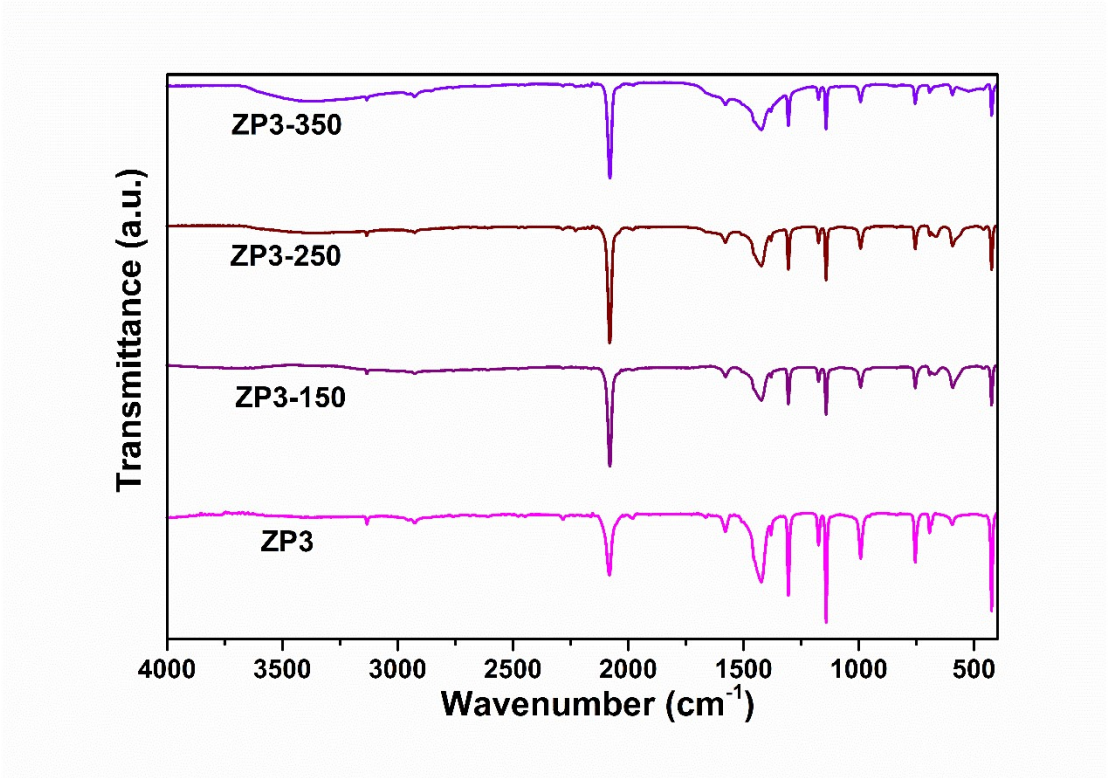


Figure S5 FT-IR spectra of the ZP1, ZP1-150, ZP1-250, ZP1-350 composites.

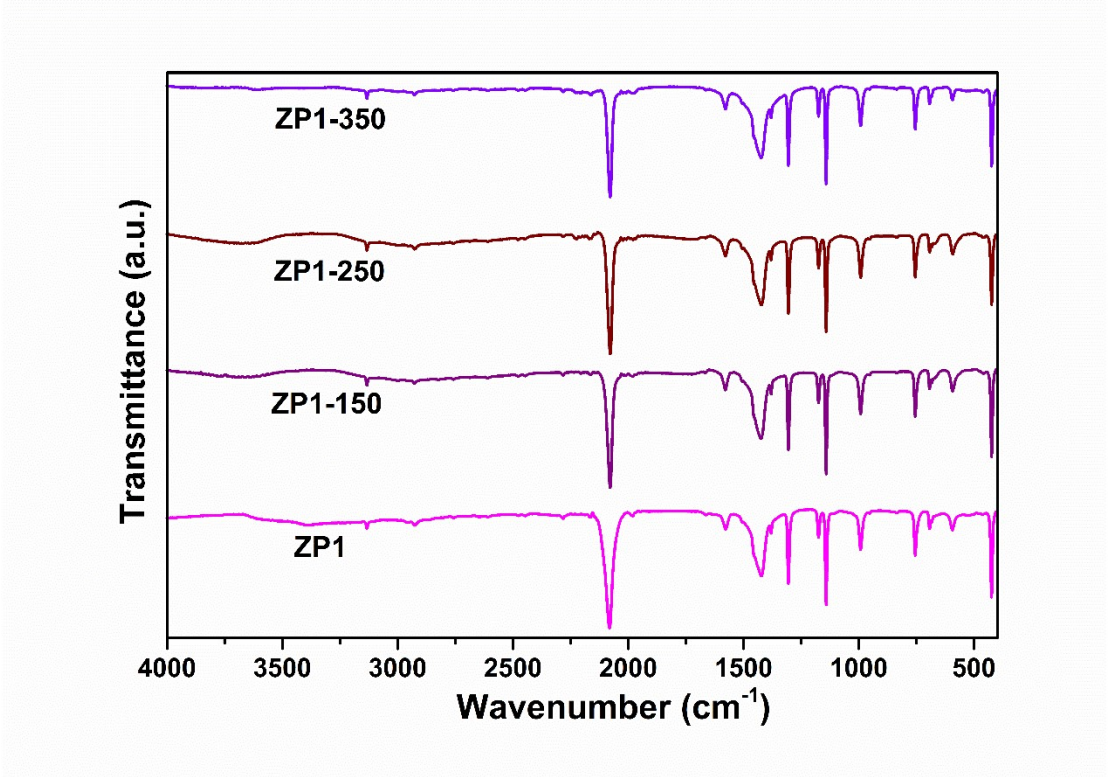


Figure S6 FT-IR spectra of the ZP3, ZP3-150, ZP3-250, ZP3-350 composites.

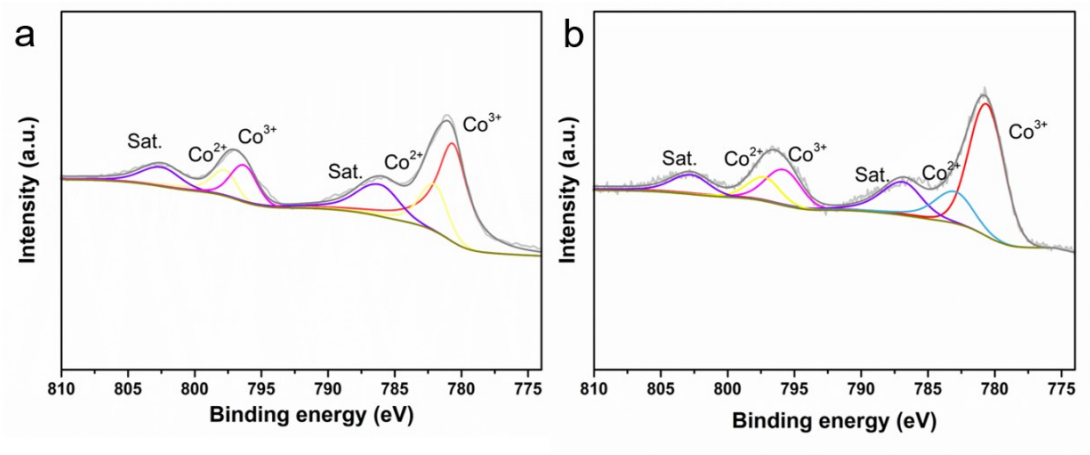


Figure S7 High-resolution Co 2p XPS spectra of (a) ZP2-150, (b) ZP2-350 composites.

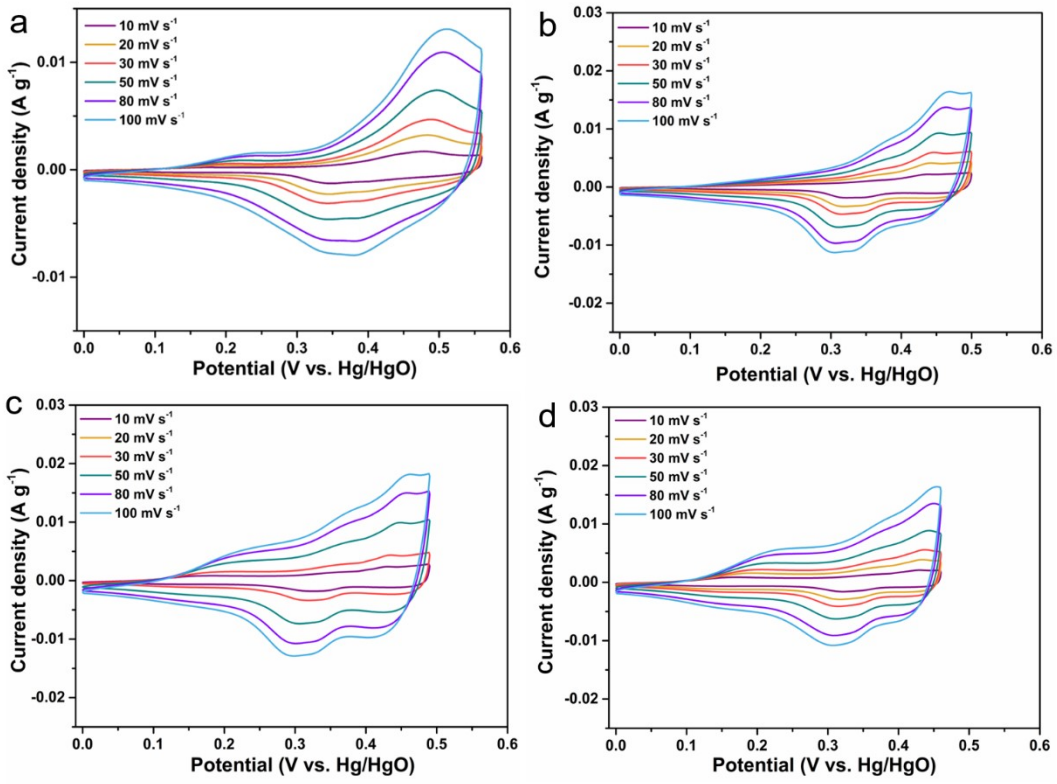


Figure S8 The electrochemical performance of the (a) ZP1, (b) ZP1-150, (c) ZP1-250, (d) ZP1-350 in a three-electrode cell: the CV curves at different current densities.

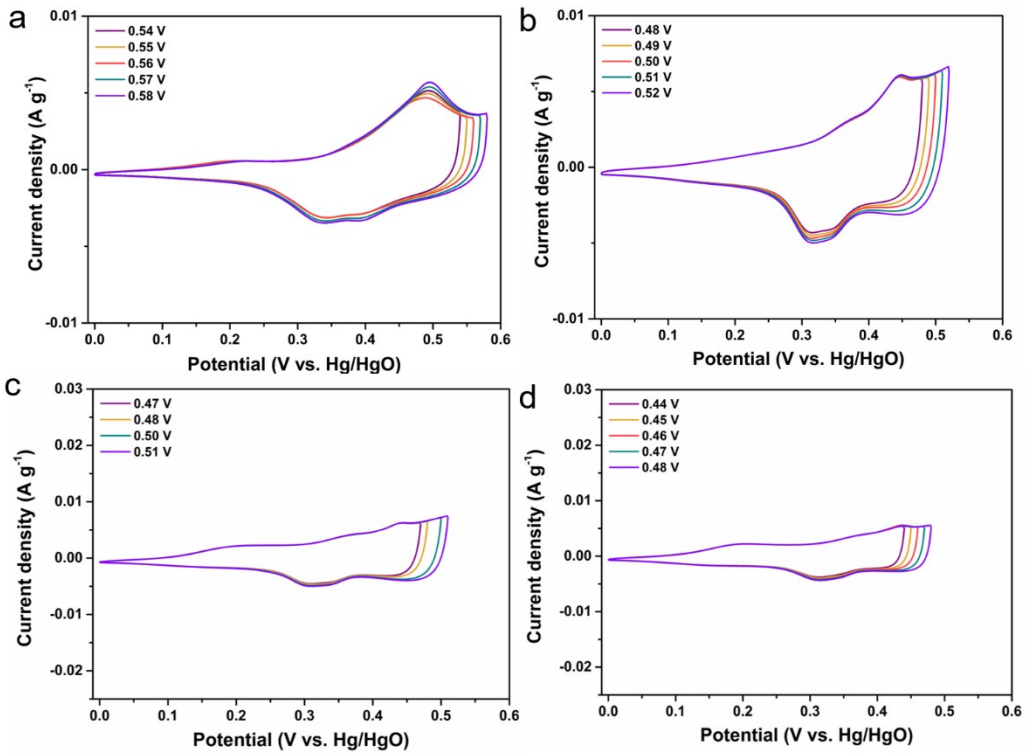


Figure S9 The electrochemical performance of the (a) ZP1, (b) ZP1-150, (c) ZP1-250, (d) ZP1-350 in a three-electrode cell: the CV curves with a scan rate at 30 mV $s^{-1}$ at different potentials.

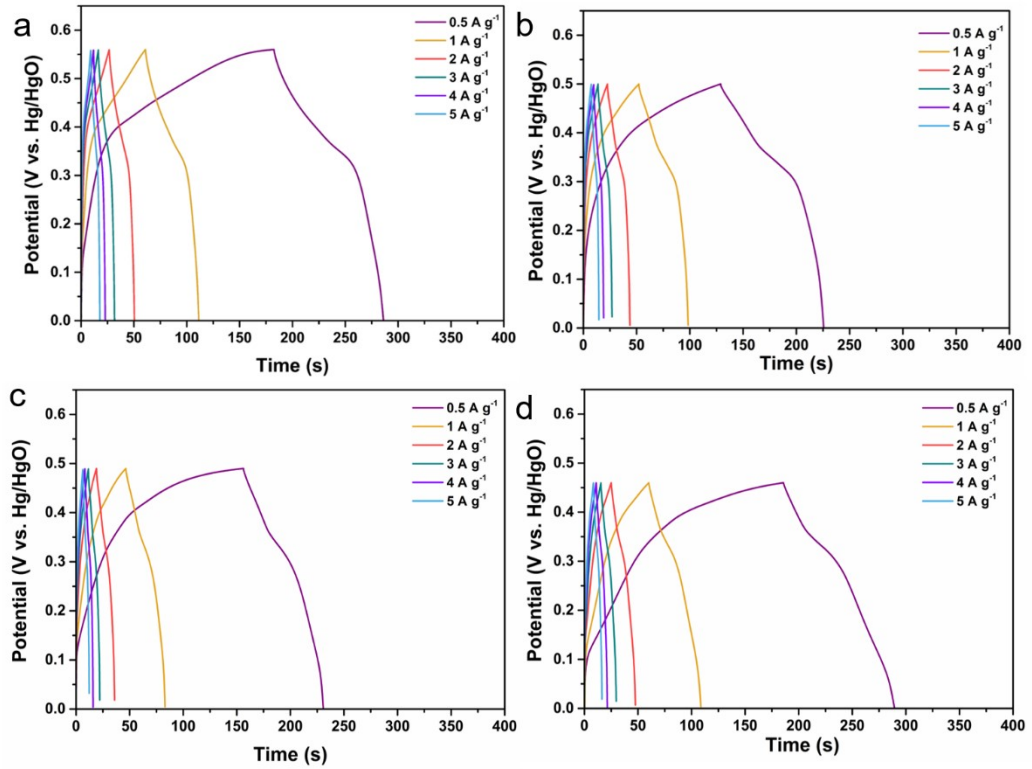


Figure S10 The electrochemical performance of the (a) ZP1, (b) ZP1-150, (c) ZP1-250, (d) ZP1-350 in a three-electrode cell: the GCD curves at different current densities.

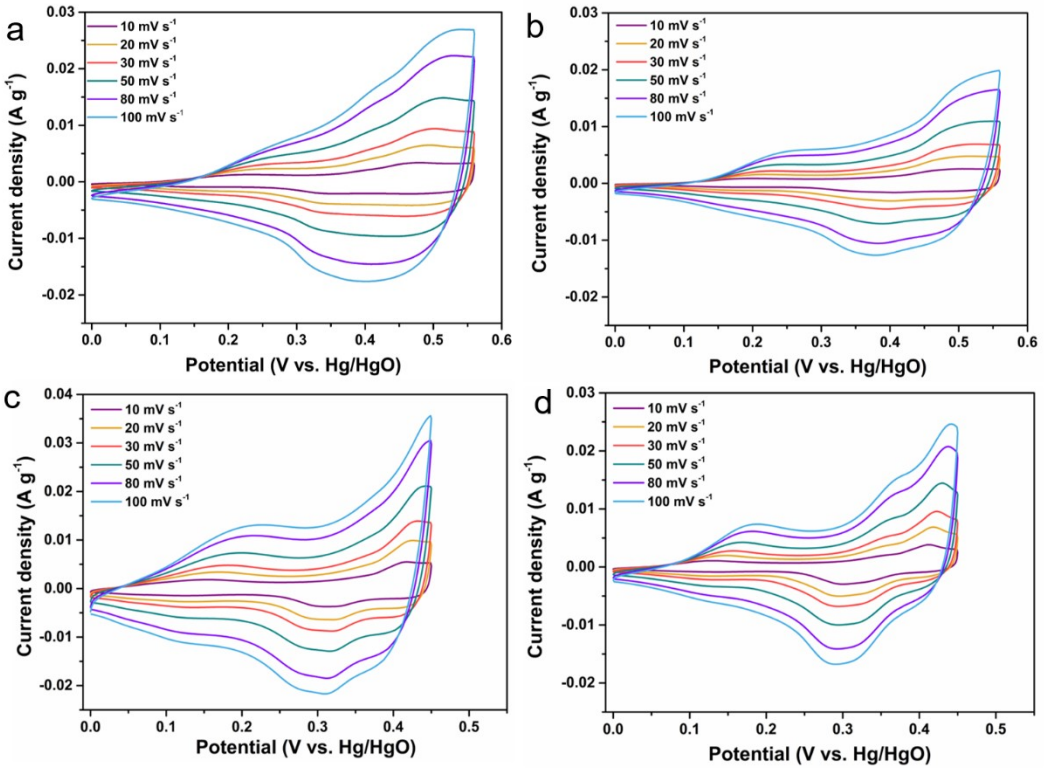


Figure S11 The electrochemical performance of the (a) ZP2, (b) ZP2-150, (c) ZP2-250, (d) ZP2-350 in a three-electrode cell: the CV curves at different current densities.

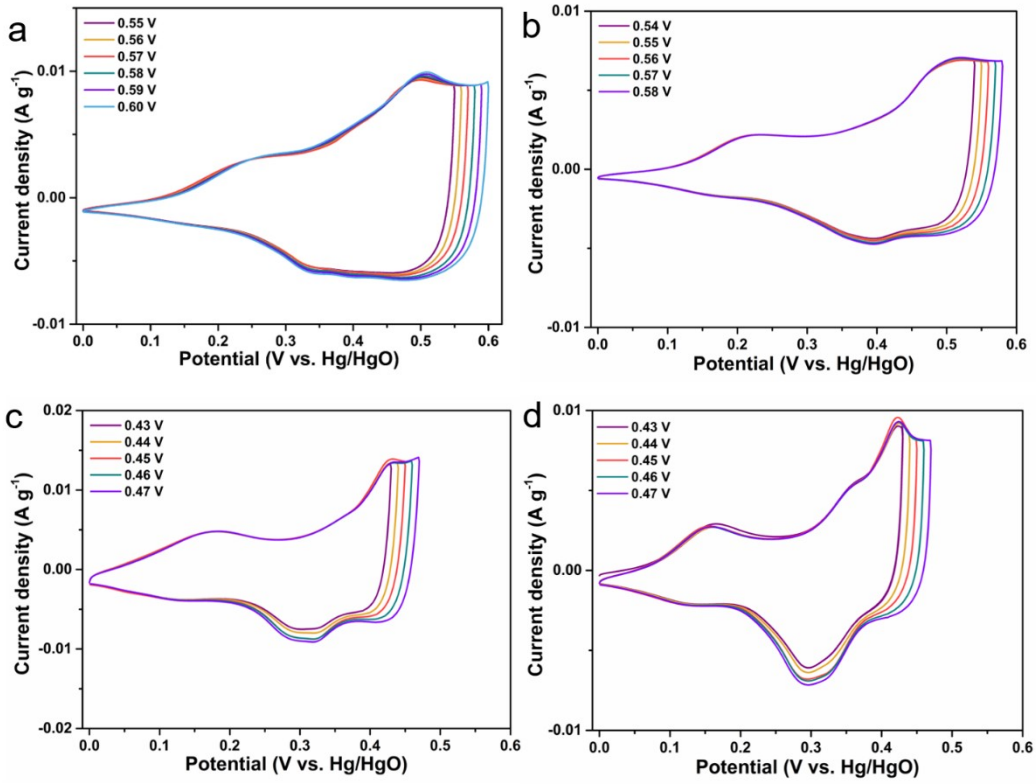


Figure S12 The electrochemical performance of the (a) ZP2, (b) ZP2-150, (c) ZP2-250, (d) ZP2-350 in a three-electrode cell: the CV curves with a scan rate at 30 mV $s^{-1}$ at different potentials.

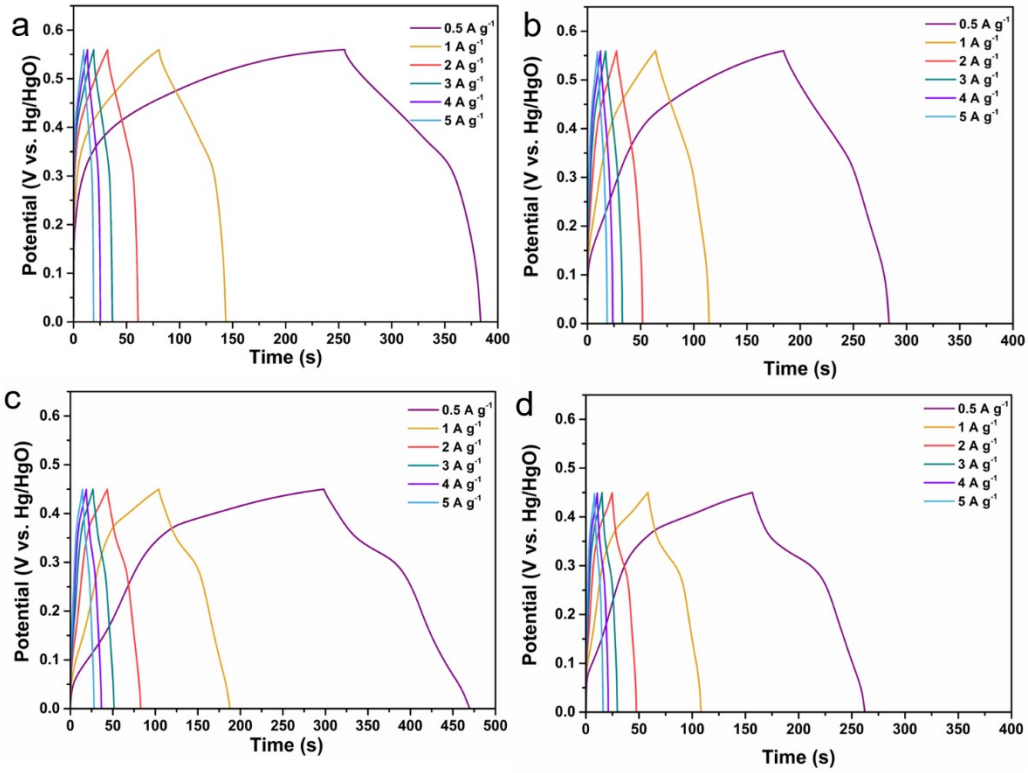


Figure S13 The electrochemical performance of the (a) ZP2, (b) ZP2-150, (c) ZP2-250, (d) ZP2-350 in a three-electrode cell: the GCD curves at different current densities.

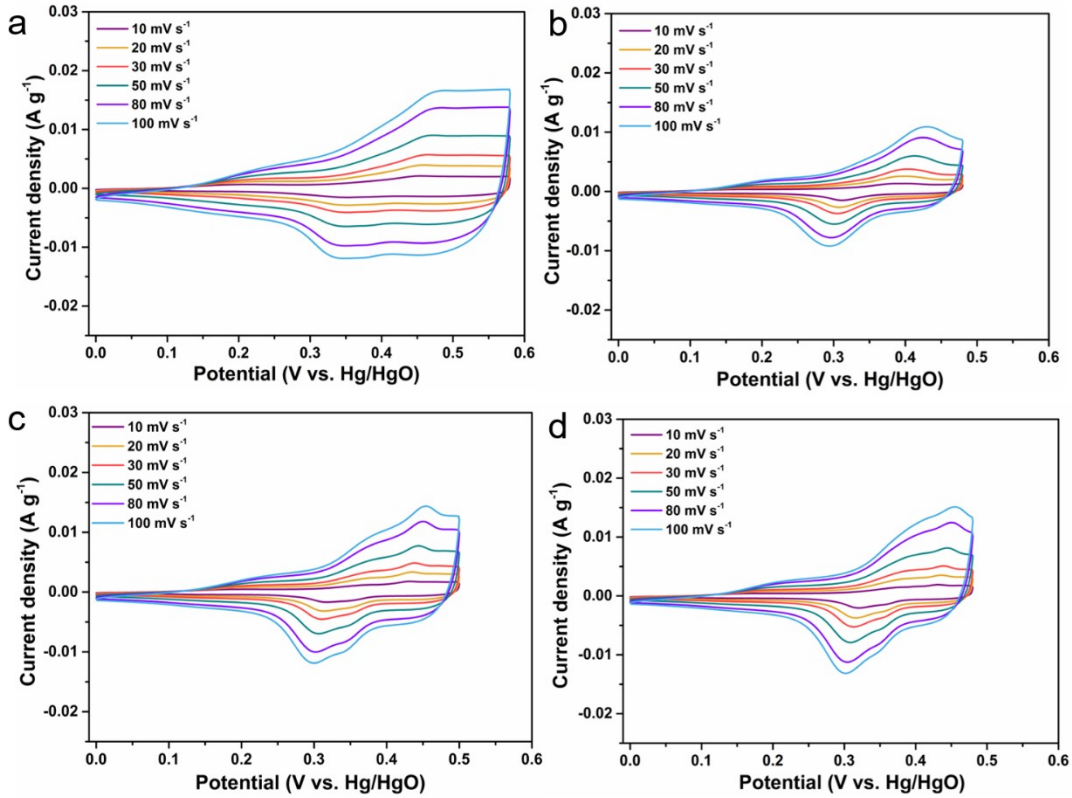


Figure S14 The electrochemical performance of the (a) ZP3, (b) ZP3-150, (c) ZP3-250, (d) ZP3-350 in a three-electrode cell: the CV curves at different current densities.

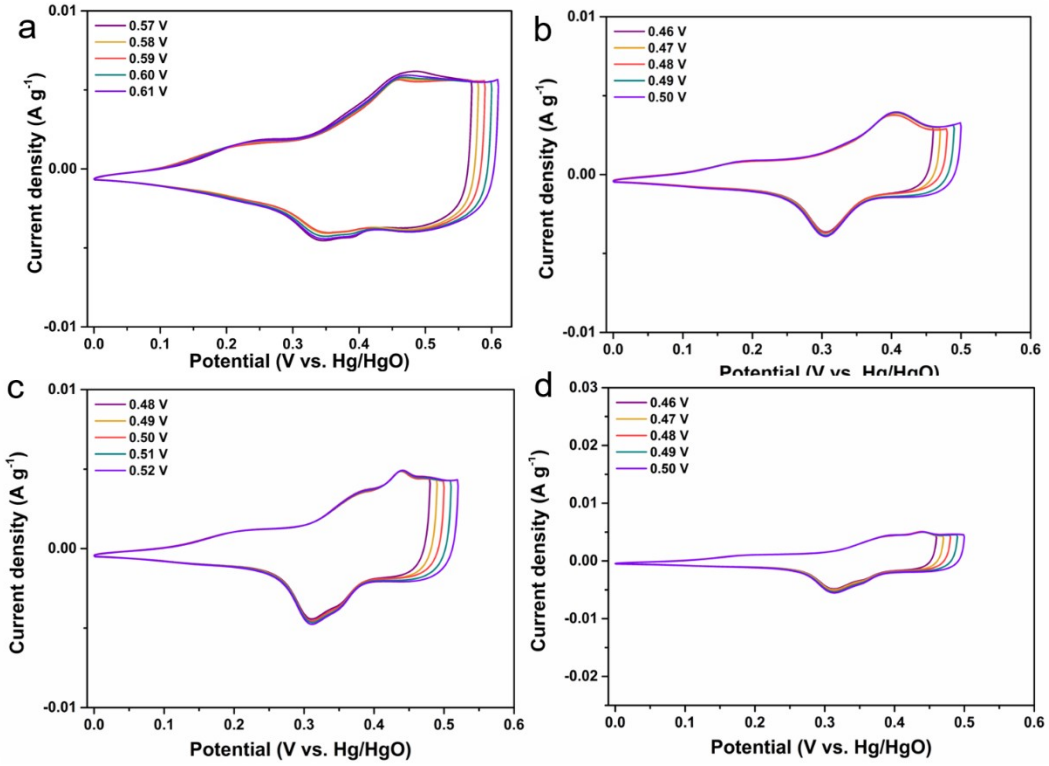


Figure S15 The electrochemical performance of the (a) ZP3, (b) ZP3-150, (c) ZP3-250, (d) ZP3-350 in a three-electrode cell: the CV curves with a scan rate at 30 mV $s^{-1}$ at different potentials.

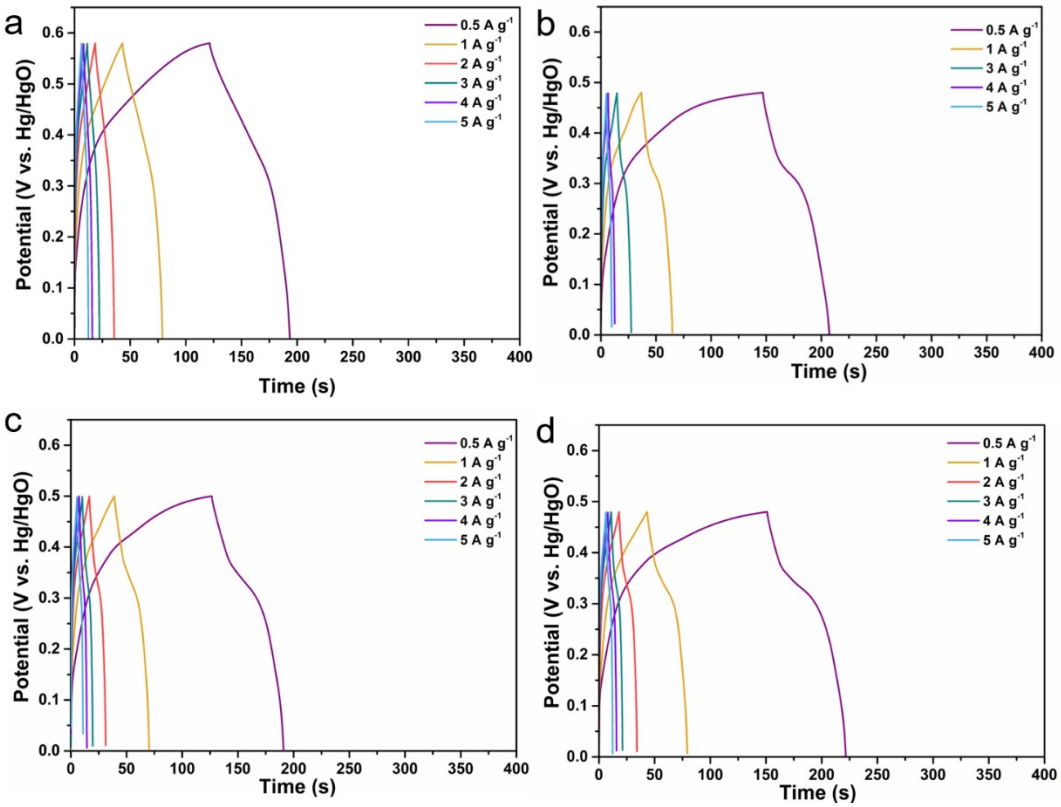


Figure S16 The electrochemical performance of the (a) ZP3, (b) ZP3-150, (c) ZP3-250, (d) ZP3-350 in a three-electrode cell: the GCD curves at different current densities.

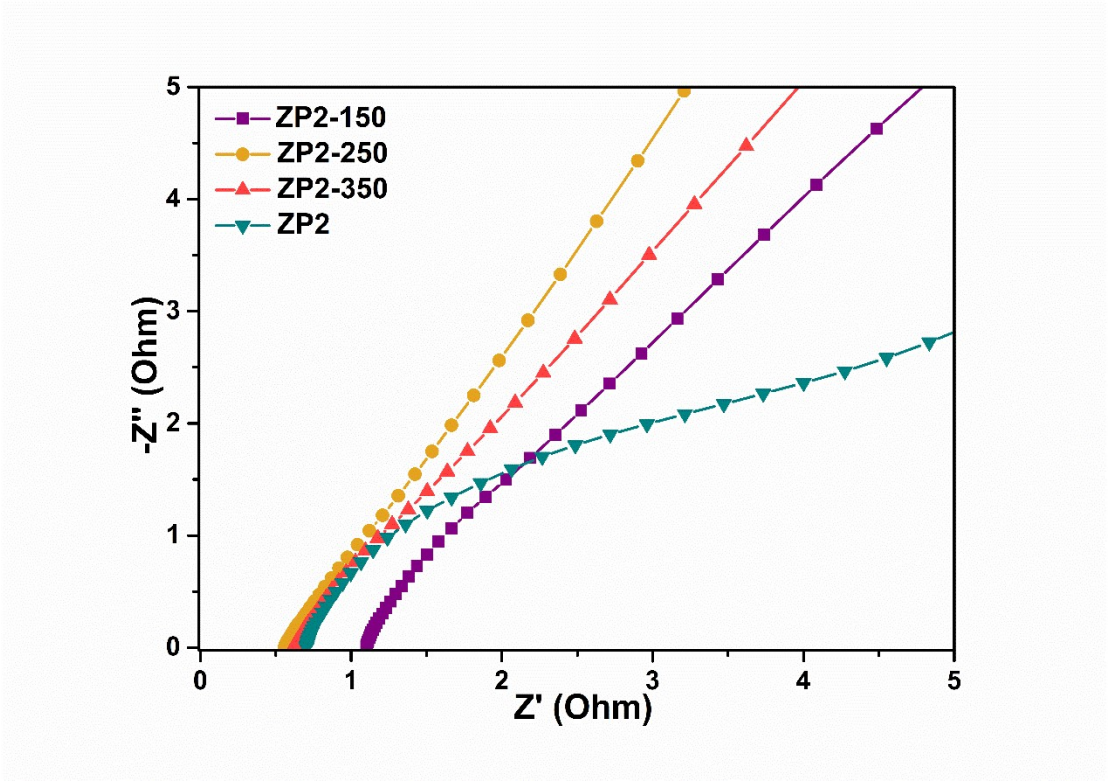


Figure S17 The EIS of the ZP2, ZP2-150, ZP2-250, ZP2-350 composites in three-electrode system.

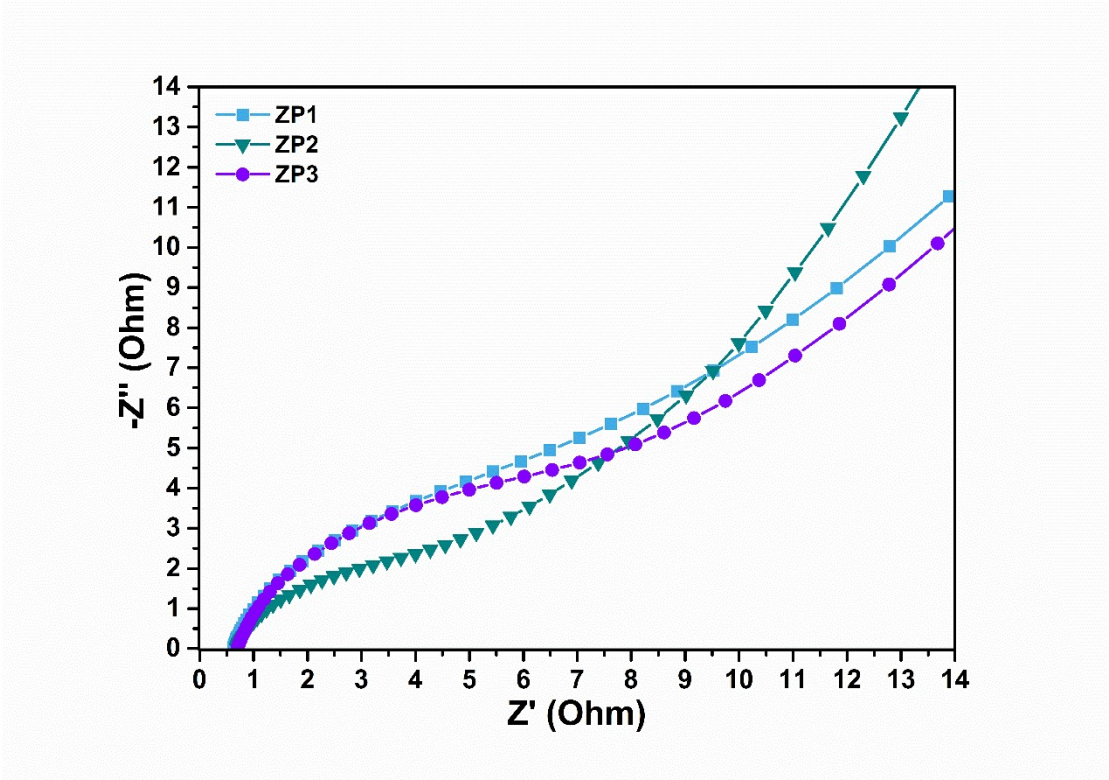


Figure S18 The EIS of the ZP1, ZP2, ZP3 composites in three-electrode system.

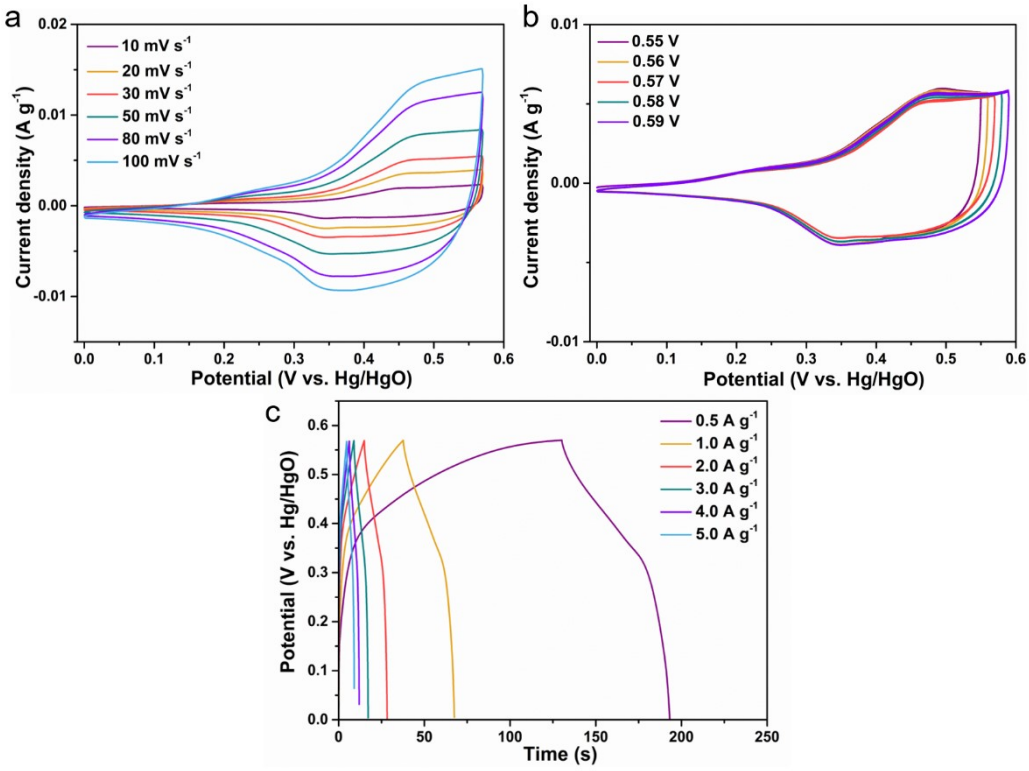


Figure S19 The electrochemical performance of the ZIF-67 :(a) the CV curves at different current densities; (b) the CV curves with a scan rate at 30 mV $s^{-1}$ at different potentials; (c) the GCD curves at different current densities.

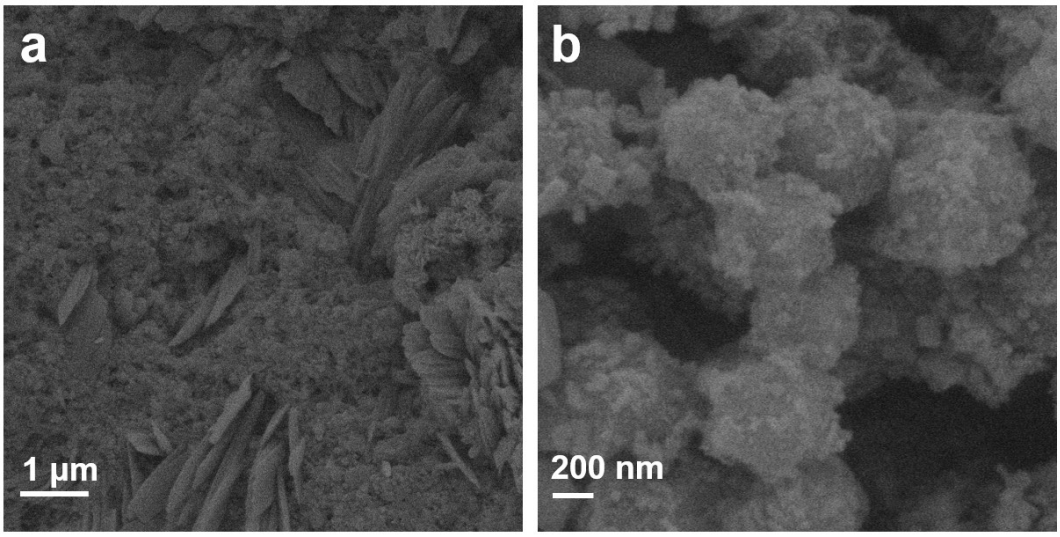


Figure S20 The SEM images of ZP2-250 electrode after long cycles.

## Reference


1 V. Shrivastav, S. Sundriyal, A. Kaur, U. K. Tiwari, S. Mishra and A. Deep, Conductive and Porous ZIF-67/PEDOT Hybrid Composite as Superior Electrode for All-Solid-State Symmetrical Supercapacitors. *J. Alloys Compd.*, 2020, **843**, 155992.

2 W. Cao, M. Han, L. Qin, Q. Jiang, J. Xu, Z. Lu and Y. Wang, Synthesis of Zeolitic Imidazolate Framework-67 Nanocube Wrapped by Graphene Oxide and Its Application for Supercapacitors. *J. Solid State Electrochem.*, 2019, **23**, 325–334.

3 Z. Ma, J. Li, R. Ma, J. He, X. Song, Y. Yu, Y. Quan and G. Wang, The Methodologically Obtained Derivative of ZIF-67 Metal-Organic Frameworks Present Impressive Supercapacitor Performance. *New J. Chem.*, 2022, **46**, 7230–7241.

4 D. Zhang, H. Shi, R. Zhang, Z. Zhang, N. Wang, J. Li, B. Yuan, H. Bai and J. Zhang, Quick Synthesis of Zeolitic Imidazolate Framework Microflowers with Enhanced Supercapacitor and Electrocatalytic Performances. *RSC Adv.*, 2015, **5**, 58772–58776.